Nonlinear data-driven model order reduction applied to circuit-field magnetic problem

Antoine Pierquin, Thomas Henneron

Nonlinear data-driven model order reduction applied to circuit-field magnetic problem

Antoine Pierquin[1] and Thomas Henneron[2],
[1]Institute for Research in Electrical Energy of Nantes-Atlantique (IREENA), Univ. Nantes, 44602 Saint-Nazaire, France
[2]Univ. Lille, Centrale Lille, Arts et Metiers ParisTech, HEI, EA 2697 - L2EP, F-59000 Lille, France

As in most of the domains in physics, finite element formulation is a very common method for electromagnetic fields computation. Since many years both proper orthogonal decomposition and empirical interpolation method are also often used in a model order reduction context. If these methods are efficients, their application is intrusive because it requires an access to the matrices and the assembly step. To avoid such an aspect, a data-driven model order reduction based on proper orthogonal decomposition with an approximation of the nonlinear terms by radial basis functions interpolation is applied to a magnetostatic problem coupled with circuit equations. The nonlinear reduced order model only needs solutions of a finite element analysis to be generated.

***Index Terms*—nonlinear magnetic problem, model order reduction, data driven**

I. Introduction

MODEL order reduction (MOR) approaches are widely used in all the engineering sciences to decrease simulations durations of complex systems [1], [2]. In electromagnetic fields computation, MOR methods are often applied to finite element (FE) problems using proper generalized decomposition [4]–[6], Padé expansion [7], proper orthogonal decomposition [3], [8], [9],... Among these methods the proper orthogonal decomposition (POD) is probably one of the most popular. Based on the solutions (called snapshots) of the FE simulation for different values of parameters, the POD enables to approximate the solution of the FE problem in a reduced basis. Then the initial FE system is projected onto the reduced basis decreasing the number of degrees of freedom to find for new parameter values. However this method is intrusive in the sense that an access to the matrix of the FE system is needed. Moreover in the nonlinear case, POD is classically combined with empirical interpolation method (EIM) [10], [11] which is even more intrusive since an access to the assembly process of the nonlinear terms is required. Indeed this method consists in interpolating the nonlinear terms of the full model by calculating only some of their entries. Consequently inference based or data-driven MOR strategies [12]–[15] are interesting because they are non intrusive and allow to obtain a reduced model only from full model solutions. Nevertheless, if data-driven strategy is well defined when the non-linear expression is clearly identified [12], it could be more complex to deal with if the nonlinear behaviour is not known. In this article we investigate a data-driven strategy for model order reduction of an electromagnetic device simulated by FE analysis with no *a priori* knowledge of the nonlinear expression, this expression being treated in a more general way using an interpolation method.

We consider the Maxwell equations in magnetostatics low frequency case: displacement current density is neglected, no eddy current is considered and a current density source is imposed through a winding. The common A-formulation is appplied to express magnetic induction from a vector potential. Moreover Maxwell equations are coupled with circuit equations where the magnetic flux is linked with winding's resistance, winding's current and a voltage source, introducing a time dependancy. From this problem a data-driven method is developped. The data-driven method is based on POD with an approximation of the nonlinear terms based on radial basis functions (RBF) interpolation [16]. The reduced order model (ROM) is obtained from snapshots of classical tests, at no load and in short circuit, usually used in electrical engineering to characterize an electromagnetic device. The POD is applied on the snapshots, after what the reduced matrices are identified using operator inference [12], [13]. The key point of the proposed method is to be able to finally approximate the reduced nonlinear terms without any *a priori* knowledge or hypothesis about it, using RBF interpolation.

The contents of this article is as follows. Firstly the problem statement and the variationnal formulation are introduced. Secondly the model order reduction method is developped with details about proper orthogonal decomposition, operator inference and nonlinear terms interpolation. Finally in an offline/online context [19], [20] the ROM generated offline should be able to simulate a different case online. Consequently the reduction strategy is applied on a 3D transformer simulation with validations on different load connected to the device.

II. Nonlinear circuit-field magnetic problem

Let consider the circuit-field magnetic problem on a domain Ω with a magnetic subdomain Ω_m and n_i windings (figure 1) such that

$$\nabla \times H = \sum_{k=1}^{n_i} J_k \tag{1}$$

with H the magnetic field and J_k the current density vector source in the k-th winding. From the conservative law $\nabla.B = 0$, the magnetic induction B is expressed as $B = \nabla \times A$ with A the vector potential. Moreover in the ferromagnetic material,

Manuscript received ???; revised ???. Corresponding author: A. Pierquin (email: antoine.pierquin@univ-nantes.fr).

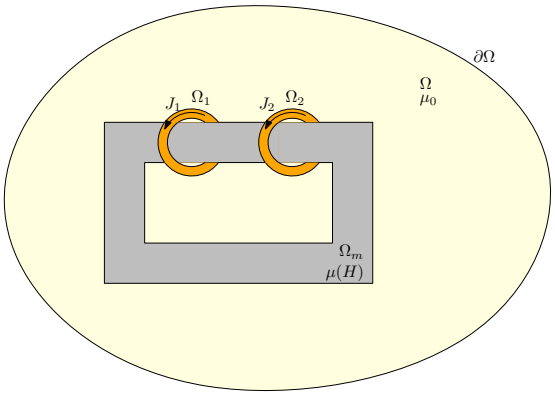

Fig. 1. Domain and subdomains of the problem.

the permeability μ is nonlinear depending on the magnetic field H in the constitutive law $B = \mu(H)H$; otherwise the law is $B = \mu_0 H$ with μ_0 the vacuum permeability. In the case of A formulation, it is necessary to express H as a function of B. Then, magnetic field is espressed as $H = \nu(B)B$ with $\nu(B)$ the reluctivity. The boundary condition $B.n = 0$ is imposed on $\partial\Omega$, with n the outgoing normal vector. Consequently the Ampere's law (1) rewrites

$$\nabla \times [\nu(B)\nabla \times A] = \sum_{k=1}^{n_i} J_k. \tag{2}$$

The current density vector is imposed in the n_i inductors by $J_k = \dfrac{T_k i_k}{S_k} D_k$ with T_k the number of turns, i_k the current, S_k the equivalent surface and D_k the normalised current direction for the k-th stranded inductor.

The magnetic flux allows to couple the local equation (1) with circuit equation by adding the n_i equalities

$$\frac{\mathrm{d}\phi_k(t)}{\mathrm{d}t} + R_k i_k(t) = v_k(t) \tag{3}$$

with ϕ_k the magnetic linkage flux, R_k the winding's resistance and v_k the source voltage for the k-th inductor.

Applying a variationnal formulation (1) leads to [23]

$$\begin{aligned} \left(\nabla \times [\nu(B)\nabla \times A], A'\right)_\Omega &= \sum_{k=1}^{n_i} \left(J_k, A'\right)_{\Omega_k} \\ \Rightarrow \left(\nu(B)\nabla \times A, \nabla \times A'\right)_\Omega &+ \left(A', n \times H\right)_{\partial\Omega} = \\ &\sum_{k=1}^{n_i} \left(J_k, A'\right)_{\Omega_k}, \end{aligned} \tag{4}$$

where $(.,.)$ is the dot product and A' the test function. The contour integral onto $\partial\Omega$ will vanish by imposing $A \times n = 0$ on $\partial\Omega$ to satisfy $B.n = 0$, with n the outgoing normal vector. The nonlinear term can be transfered only on the right-hand-side such that

$$\begin{aligned} \left(\nu_0 \nabla \times A, \nabla \times A'\right)_\Omega &= \sum_{k=1}^{n_i} \left(J_k, A'\right)_{\Omega_k} \\ &- \left((\nu(B) - \nu_0)\nabla \times A, \nabla \times A'\right)_\Omega, \end{aligned} \tag{5}$$

with ν_0 the slope of ν in 0.

Adding to these expressions the circuit equations (3) in each winding where the magnetic linkage flux ϕ_k can be expressed as a function of A by [21], [22]

$$\phi_k = \left(\frac{T_k}{S_k} D_k, A\right)_\Omega, \tag{6}$$

Finally after a Ritz-Galerkin discretization we obtain for linear case the system

$$\begin{cases} \mathbf{M}\mathbf{X}(t) - \mathbf{F}\mathbf{I}(t) = 0, \\ \mathbf{F}^t \dfrac{\mathrm{d}\mathbf{X}(t)}{\mathrm{d}t} + \mathbf{R}\mathbf{I}(t) = \mathbf{V}(t), \end{cases} \tag{7}$$

and for nonlinear case

$$\begin{cases} \mathbf{M}\tilde{\mathbf{X}}(t) - \mathbf{F}\tilde{\mathbf{I}}(t) = \mathbf{G}(\tilde{\mathbf{X}}(t)), \\ \mathbf{F}^t \dfrac{\mathrm{d}\tilde{\mathbf{X}}(t)}{\mathrm{d}t} + \mathbf{R}\tilde{\mathbf{I}}(t) = \mathbf{V}(t), \end{cases} \tag{8}$$

with $\mathbf{X} \in \mathbb{R}^{n_x}$ and $\tilde{\mathbf{X}} \in \mathbb{R}^{n_x}$ the circulations of potential vector A for all edges of the mesh, $\mathbf{I} \in \mathbb{R}^{n_i}$ and $\tilde{\mathbf{I}} \in \mathbb{R}^{n_i}$ the vector of winding currents, $\mathbf{V} \in \mathbb{R}^{n_i}$ the source voltage vector. $\mathbf{M} \in \mathbb{R}^{n_x \times n_x}$ is the "curl-curl" matrix such that

$$M_{\ell,k} = \int_\Omega \nu_0 \nabla \times w_\ell \cdot \nabla \times w_k \, \mathrm{d}\Omega, \tag{9}$$

with $(w_k)_{k=1,\dots,n_x}$ the edge shape functions. The nonlinear vector is such that

$$G_\ell(\tilde{\mathbf{X}}(t)) = \sum_{k=1}^{n_x} \int_\Omega (\nu(B) - \nu_0)\nabla \times w_\ell \cdot \nabla \times w_k \tilde{X}_k(t) \, \mathrm{d}\Omega, \tag{10}$$

$\mathbf{R} \in \mathbb{R}^{n_i \times n_i}$ is the diagonal matrix of resistor and $\mathbf{F} \in \mathbb{R}^{n_x \times n_i}$ the matrix

$$F_{\ell,k} = \int_\Omega \frac{T_k}{S_k} D_k \cdot \nabla \times w_\ell \, \mathrm{d}\Omega, \tag{11}$$

such that the magnetic fluxes can be expressed by

$$\mathbf{\Phi}(t) = \mathbf{F}^t \mathbf{X}(t) \in \mathbb{R}^{n_i} \tag{12}$$

and

$$\tilde{\mathbf{\Phi}}(t) = \mathbf{F}^t \tilde{\mathbf{X}}(t) \in \mathbb{R}^{n_i}, \tag{13}$$

discrete forms of equation (6).

III. Nonlinear data-driven model order reduction

Both linear and nonlinear problems (7)-(8) are solved using a time stepping scheme to obtain n_s solutions $\mathbf{X}(t_k)$, $\mathbf{I}(t_k)$ and $\tilde{\mathbf{X}}(t_k)$, $\tilde{\mathbf{I}}(t_k)$ for time steps t_k with $k = 1$ to n_s. The associated flux $\mathbf{\Phi}(t_k)$ and $\tilde{\mathbf{\Phi}}(t_k)$ are also computed. The solutions are stored in snapshot matrices with

$$\mathbf{S}_\mathbf{X} = \left[\mathbf{X}(t_1), \mathbf{X}(t_2), \dots, \mathbf{X}(t_{n_s})\right] \in \mathbb{R}^{n_x \times n_s} \tag{14}$$

$$\mathbf{S}_\mathbf{I} = \left[\mathbf{I}(t_1), \mathbf{I}(t_2), \dots, \mathbf{I}(t_{n_s})\right] \in \mathbb{R}^{n_i \times n_s} \tag{15}$$

$$\mathbf{S}_\mathbf{\Phi} = \left[\mathbf{\Phi}(t_1), \mathbf{\Phi}(t_2), \dots, \mathbf{\Phi}(t_{n_s})\right] \in \mathbb{R}^{n_i \times n_s} \tag{16}$$

$$\mathbf{S}_{\tilde{\mathbf{X}}} = \left[\tilde{\mathbf{X}}(t_1), \tilde{\mathbf{X}}(t_2), \dots, \tilde{\mathbf{X}}(t_{n_s})\right] \in \mathbb{R}^{n_x \times n_s} \tag{17}$$

$$\mathbf{S}_{\tilde{\mathbf{I}}} = \left[\tilde{\mathbf{I}}(t_1), \tilde{\mathbf{I}}(t_2), \dots, \tilde{\mathbf{I}}(t_{n_s})\right] \in \mathbb{R}^{n_i \times n_s} \tag{18}$$

$$\mathbf{S}_{\tilde{\mathbf{\Phi}}} = \left[\tilde{\mathbf{\Phi}}(t_1), \tilde{\mathbf{\Phi}}(t_2), \dots, \tilde{\mathbf{\Phi}}(t_{n_s})\right] \in \mathbb{R}^{n_i \times n_s} \tag{19}$$

The matrix $\mathbf{R}$ is known and the number of currents is small so the reduction will be applied only on the vectors $\mathbf{X}$ and $\tilde{\mathbf{X}}$.

A. Proper orthogonal decomposition

A first reduced basis $\mathbf{\Psi}$ is computed using proper orthogonal decomposition (POD) from $\mathbf{S_X}$ and a second ones $\tilde{\mathbf{\Psi}}$ from $\mathbf{S_{\tilde{X}}}$. The POD consists in applying a singular value decomposition (SVD) to $\mathbf{S_X}$ and $\mathbf{S_{\tilde{X}}}$ to obtain the decompositions

$$\mathbf{S_X} = \mathbf{U_X \Sigma_X W_X}^t \quad \text{with} \quad \mathbf{S_{\tilde{X}}} = \mathbf{U_{\tilde{X}} \Sigma_{\tilde{X}} W_{\tilde{X}}}^t, \tag{20}$$

with $\mathbf{U_X}, \mathbf{U_{\tilde{X}}} \in \mathbb{R}^{n_x \times n_x}$ and $\mathbf{W_X}, \mathbf{W_{\tilde{X}}} \in \mathbb{R}^{n_s \times n_s}$ orthonormal matrices and $\mathbf{\Sigma_X}, \mathbf{\Sigma_{\tilde{X}}} \in \mathbb{R}^{n_x \times n_s}$ diagonal matrices of singular values $\sigma_{\mathbf{X},k}$ and $\sigma_{\mathbf{\tilde{X}},k}$, $k = 1$ to n_s. The projection matrices $\mathbf{\Psi}$ and $\tilde{\mathbf{\Psi}}$ are made of the first columns of $\mathbf{U_X}$ and $\mathbf{U_{\tilde{X}}}$ respectively, the number of columns being chosen most of the time using the singular values by the following energetic criterion

$$\frac{\sum_{k=1}^{r_\mathbf{X}} \sigma_{\mathbf{X},k}}{\sum_{k=1}^{n_s} \sigma_{\mathbf{X},k}} \leq 1 - \varepsilon \quad \text{and} \quad \frac{\sum_{k=1}^{r_{\tilde{\mathbf{X}}}} \sigma_{\mathbf{\tilde{X}},k}}{\sum_{k=1}^{n_s} \sigma_{\mathbf{\tilde{X}},k}} \leq 1 - \varepsilon, \tag{21}$$

with ε a given tolerance.

Once $\mathbf{\Psi}$ and $\tilde{\mathbf{\Psi}}$ are computed then the final basis $\mathbf{P} \in \mathbb{R}^{n_x \times n_r}$ is obtained by a third SVD on the concatenated matrix $\mathbf{S} = \left[\mathbf{\Psi}, \tilde{\mathbf{\Psi}}\right] \in \mathbb{R}^{n_x \times r_S}$ with $r_s = r_\mathbf{X} + r_{\tilde{\mathbf{X}}}$ in order to optimize the size of the basis. Once again $\mathbf{S} = \mathbf{U \Sigma W}^t$ with $\mathbf{U} \in \mathbb{R}^{n_x \times n_x}$ and $\mathbf{W} \in \mathbb{R}^{r_s \times r_s}$ orthonormal matrices and $\mathbf{\Sigma} \in \mathbb{R}^{n_x \times r_s}$ a diagonal matrix of singular values σ_k, $k = 1$ to r_s. Finally $\mathbf{P}$ is made of the n_r first columns of $\mathbf{U}$, the choice of n_r being based on the same criterion

$$\frac{\sum_{k=1}^{n_r} \sigma_k}{\sum_{k=1}^{n_s} \sigma_k} \leq 1 - \varepsilon. \tag{22}$$

The reduced basis is used to perform projection of the solutions onto the reduced space by

$$\mathbf{s_x} = \mathbf{P}^t \mathbf{S_X} = \left[\mathbf{x}_1, \mathbf{x}_2, \ldots, \mathbf{x}_{n_s}\right] \in \mathbb{R}^{n_r \times n_s} \tag{23}$$

for the linear solutions and

$$\mathbf{s_{\tilde{x}}} = \mathbf{P}^t \mathbf{S_{\tilde{X}}} = \left[\tilde{\mathbf{x}}_1, \tilde{\mathbf{x}}_2, \ldots, \tilde{\mathbf{x}}_{n_s}\right] \in \mathbb{R}^{n_r \times n_s} \tag{24}$$

for the nonlinear ones.

B. Operators inference

The first aim is to obtain the reduced matrices $\mathbf{f} \in \mathbb{R}^{n_r \times n_i}$ and $\mathbf{m} \in \mathbb{R}^{n_r \times n_r}$, reduced forms of $\mathbf{M}$ and $\mathbf{F}$ by Galerkin projection, respectively

$$\mathbf{m} \simeq \mathbf{P}^t \mathbf{M P}, \tag{25}$$

$$\mathbf{f} \simeq \mathbf{P}^t \mathbf{F}. \tag{26}$$

To do so we consider that the reduced vectors $\mathbf{x}_k$ from $\mathbf{s_x}$ must verify [12], [13], [15]

$$\mathbf{f}^t \mathbf{x}(t_k) = \mathbf{\Phi}(t_k) \quad \forall k \in \{1, \ldots, n_s\} \tag{27}$$

$$\text{and} \quad \mathbf{m x}(t_k) = \mathbf{f I}(t_k) \quad \forall k \in \{1, \ldots, n_s\}, \tag{28}$$

reduced expressions of (12) and the first equation of (7).

Equation (27) can be written with snapshots matrices as $\mathbf{f}^t \mathbf{s_x} = \mathbf{S_\Phi}$ and by applying transpose operator ${\mathbf{s_x}}^t \mathbf{f} = {\mathbf{S_\Phi}}^t$. Consequently a minimization problem allows to obtain the matrix $\mathbf{f}$ because $\mathbf{f}_k$, k-th column of $\mathbf{f}$, is solution of the problem

$$\min_{\mathbf{y} \in \mathbb{R}^{n_r}} \|{\mathbf{s_x}}^t \mathbf{y} - \mathbf{c}_k\|, \tag{29}$$

with $\mathbf{c}_k$ the k-th column of ${\mathbf{S_\Phi}}^t$ which is

$$\mathbf{c}_k = \left[\phi_k(t_1), \phi_k(t_2), \ldots, \phi_k(t_{n_s})\right]^t. \tag{30}$$

In the same way (28) can be written $\mathbf{m s_x} = \mathbf{f S_I}$ or ${\mathbf{s_x}}^t \mathbf{m}^t = {\mathbf{S_I}}^t \mathbf{f}$ and so a minimization allows to obtain the matrix $\mathbf{m}$ by solving a problem as in (29) with $\mathbf{c}_k$ the k-th column of ${\mathbf{S_I}}^t \mathbf{f}$.

The least square problem (29) is basically solved by computing the pseudo-inverse of the matrix ${\mathbf{s_x}}^t$.

C. Nonlinear terms interpolation

Now that the matrices of the reduced system are known, the snapshot matrix of the reduced nonlinear term is approximated by $\mathbf{s_g} = \mathbf{m s_{\tilde{x}}} - \mathbf{f S_{\tilde{I}}} \in \mathbb{R}^{n_r \times n_s}$, containing the reduced term $\mathbf{g}$ of the nonlinear vector $\mathbf{G}$ at each time step t_k, $k = 1$ to n_s. These reduced terms will be interpolated for each component during the solving of the reduced problem to obtain an approximation of the nonlinear term depending on the vector $\mathbf{x}$ using radial basis functions (RBF). Consequently the reduced nonlinear term $\mathbf{g}$ is approximated for a reduced vector $\mathbf{x}$ by

$$\mathbf{g}(\mathbf{x}) \simeq \begin{bmatrix} \alpha_{11} & \alpha_{12} & \ldots & \alpha_{1n_s} \\ \alpha_{21} & \alpha_{22} & \ldots & \alpha_{2n_s} \\ \vdots & & & \\ \alpha_{n_r 1} & \alpha_{n_r 2} & \vdots & \alpha_{n_r, n_s} \end{bmatrix} \begin{bmatrix} r\big(\|\mathbf{x} - \mathbf{x}_1\|, a_1\big) \\ r\big(\|\mathbf{x} - \mathbf{x}_2\|, a_2\big) \\ \vdots \\ r\big(\|\mathbf{x} - \mathbf{x}_{n_s}\|, a_{n_s}\big) \end{bmatrix}, \tag{31}$$

with $\alpha_{k\ell}$, $\ell = 1$ to n_s, the interpolation coefficients associated with the k-th component of $\mathbf{g}(\mathbf{x})$ for $k = 1$ to n_r. Function $r\big(\|\mathbf{x} - \mathbf{x}_\ell\|, a_\ell\big)$ is the RBF centered on the point $\mathbf{x}_\ell$, a_ℓ a hyperparameter of the function and $\|.\|$ the 2-norm. The hyperparameter is usually chosen and imposed by the user and the same for all the functions but multiple hyperparameters are possible and their computation can be done by cross-validation [17]. The function r can classically be [16]

- Gaussian $r(x, a) = \exp\left(-\dfrac{x^2}{a^2}\right)$.
- Inverse quadratic $r(x, a) = \dfrac{1}{1 + \frac{x^2}{a^2}}$.
- Multiquadric $r(x, a) = \sqrt{1 + \dfrac{x^2}{a^2}}$.
- Inverse multiquadric $r(x, a) = \dfrac{1}{\sqrt{1 + \frac{x^2}{a^2}}}$.
- Thin plate spline $r(x) = x^2 \ln x$.

The coefficients $\alpha_{k\ell}$ are computed by solving the $n_s \times n_s$ system

$$\begin{bmatrix} r\left(\|\mathbf{x}_1-\mathbf{x}_1\|\right) & r\left(\|\mathbf{x}_2-\mathbf{x}_1\|\right) & \dots & r\left(\|\mathbf{x}_{n_s}-\mathbf{x}_1\|\right) \\ r\left(\|\mathbf{x}_1-\mathbf{x}_2\|\right) & r\left(\|\mathbf{x}_2-\mathbf{x}_2\|\right) & \dots & r\left(\|\mathbf{x}_{n_s}-\mathbf{x}_2\|\right) \\ \vdots & & & \\ r\left(\|\mathbf{x}_1-\mathbf{x}_{n_s}\|\right) & r\left(\|\mathbf{x}_2-\mathbf{x}_{n_s}\|\right) & \dots & r\left(\|\mathbf{x}_{n_s}-\mathbf{x}_{n_s}\|\right) \end{bmatrix} \begin{bmatrix} \alpha_{k1} \\ \alpha_{k2} \\ \vdots \\ \alpha_{kn_s} \end{bmatrix} = \begin{bmatrix} g_{k1} \\ g_{k2} \\ \vdots \\ g_{kn_s} \end{bmatrix} \tag{32}$$

Once the coefficients $\alpha_{k\ell}$ are known, the interpolation is fast because it just requires to compute the distance $\|x - x_k\|$ for the n_s points then the matrix-vector product (31). Always from (31), we see that n_r interpolations are performed to evaluate $\mathbf{g}(\mathbf{x})$. Among the interpolation methods, interpolation based on RBF has the advantages to be used whatever the dimension of the input coordinates and does not require a mesh. Indeed the interpolation uses the euclidian distance between the interpolated points and functions with a continuous support.

D. Reduced system solving

Finally, the system to solve is

$$\begin{cases} \mathbf{m}\tilde{\mathbf{x}}(t) - \mathbf{f}\tilde{\mathbf{i}}(t) = \mathbf{g}(\tilde{\mathbf{x}}(t)), \\ \mathbf{f}^t \dfrac{\mathrm{d}\tilde{\mathbf{x}}(t)}{\mathrm{d}t} + \mathbf{R}\tilde{\mathbf{i}}(t) = \mathbf{V}(t). \end{cases} \tag{33}$$

An implicit Euler time-scheme is applied then at each time-step a nonlinear problem is solved using a fixed-point strategy to deal with the nonlinear behaviour of the magnetic reluctivity. During the fixed-point iterative process the reduced vector $\mathbf{g}(\mathbf{x})$ is approximated by the RBF interpolation (31). It is known that fixed-point strategy is less efficient than a Newton method, however solving reduced system is very fast so the low convergence of fixed-point is not prohibitive. Moreover the RBF interpolation does not guarantee a good approximation of the derivative of the interpolated function consequently the use of the jacobian could be disadvantageous.

E. Procedure summary

Now that all the steps are detailed, the order reduction procedure can be summarised as following:

1) Solve the linear and nonlinear problems (7) and (8) for n_s time-steps.
2) Create the snapshots matrices.
3) Solve the minimization problem (29) with $\mathbf{c}_k$ the k-th column of $\mathbf{\Phi}^t$.
4) Solve the minimization problem (29) with $\mathbf{c}_k$ the k-th column of ${\mathbf{S_I}^t}\mathbf{f}$.
5) Compute the nonlinear term snapshot matrix $\mathbf{s_g} = \mathbf{ms_{\tilde{x}}} - \mathbf{fS_{\tilde{I}}}$.
6) Find the interpolation coefficients of the RBF by solving (32).
7) Solve the reduced system (33) on the whole time-domain.

IV. Applications

The data-driven strategy is applied to 3D single-phase and a three-phase 50 Hz transformers simulated using finite element solver Gsmh/GetDP [24], [25]. Considering symetries of the device, only one quarter of the transformers is simulated. The solver used an implicit Euler scheme in time with a time-step equal to 0.25 milliseconds and a Newton strategy to solve the nonlinear problem at each time step. The simulations are done on a cluster allowing a parallel solving of the matrix systems using MUMPS solver with 8 cores. The magnetic cores of both transfomers are similar. The nonlinear magnetic law is interpolated from a set of measured points [26] as shown on figure 2.

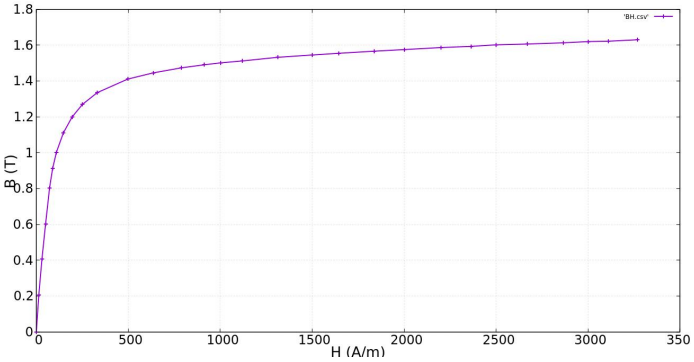

Fig. 2. Nonlinear magnetic law [26].

In order to obtain a reduced model valid on the whole operating range of transformers (i.e. for any load connected to the secondary windings), the solutions are computed for two typical configurations corresponding to extreme operating points: short-circuit to have a linear response; at no-load to have a strongly nonlinear response. Based on previous experimentations [18] the inverse multiquadric functions are used as RBF and the hyperparameter chosen is $\dfrac{1}{\sigma^2}$ with σ the standard deviation of the distances between the vectors $\tilde{x}_k$, $k = 1$ to n_s. The different POD are done with the tolerance $\varepsilon = 10^{-12}$ in equations (21)-(22).

Once the reduced model is obtained, it is simulated coupled with different loads (resistance R_c or/and inductance L_c) on a different time-window then the results are compared with a reference that is the same initial system with addition of the loads in circuit equation

$$\begin{cases} \mathbf{M}\tilde{\mathbf{X}}(t) - \mathbf{F}\tilde{\mathbf{I}}(t) = \mathbf{G}(\tilde{\mathbf{X}}(t)), \\ \mathbf{F}^t \dfrac{\mathrm{d}\tilde{\mathbf{X}}(t)}{\mathrm{d}t} + \mathbf{L}_c \dfrac{\mathrm{d}\tilde{\mathbf{I}}(t)}{\mathrm{d}t} + (\mathbf{R} + \mathbf{R_c})\tilde{\mathbf{I}}(t) = \mathbf{V}(t) \end{cases} \tag{34}$$

with $\mathbf{L}_c$ a diagonal matrix. The aim is to highlight that once the reduced model is obtained, it can be used for different configurations.

The mesh is the same for both transformers and it is made of 7808 nodes and 41224 tetrahedrons leading to 40766 unknowns in the finite element formulation. Figure 3 presents the mesh of the magnetic core and of the windings.

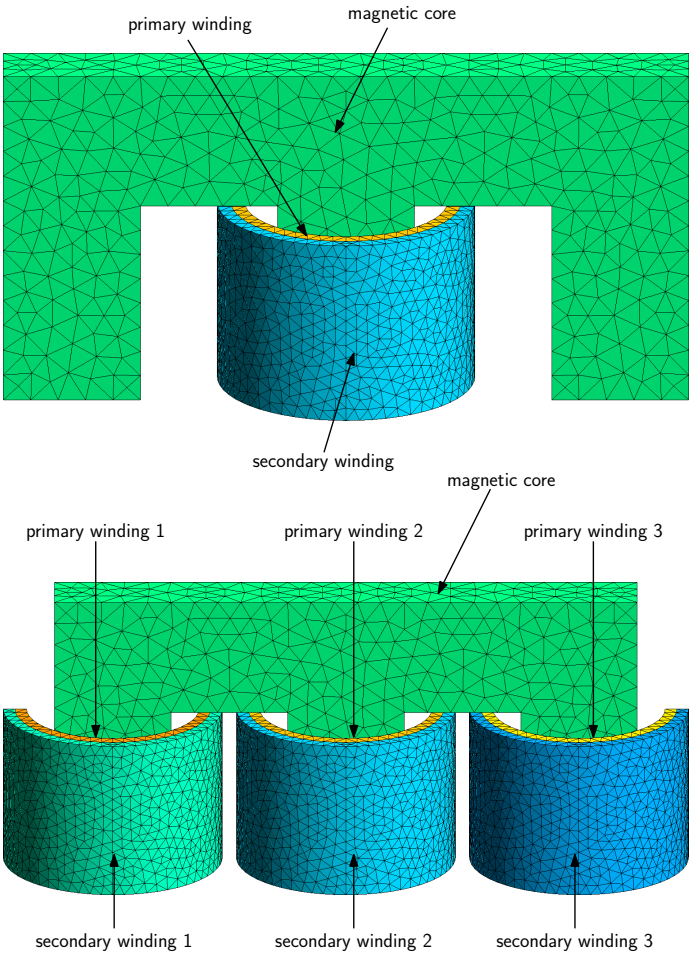

Fig. 3. Mesh of the one-phase (top) and three-phase (bottom) transformers.

A. Single-phase transformer

First the current responses are plotted figure 4 at no-load and in short-circuit. These simulations are done one the time window [0,0.06] seconds corresponding to three periods of the voltage source. The reduced order model is extracted from the solutions as explained in section III. Then the reduced order model allows to simulate the transformer coupled with a resistive load R_c equal to 30 Ω on the time window [0,0.1] seconds and a second case with resistive R_c and inductive L_c loads equal to 30 Ω and 0.1 H respectively, currents being plotted figure 5. The reduced system has 66 unknowns and the RBF interpolation is done with 160 vectors.

To compare the currents we define a temporal norm $\|\cdot\|_t$ such that

$$\|\mathbf{i}(t)\|_t = \left\| \begin{vmatrix} i(t_1) \\ i(t_2) \\ \vdots \\ i(t_n) \end{vmatrix} \right\|_2, \tag{35}$$

with $\|\cdot\|_2$ the Euclidian norm.

To compare the solution vectors we use the 2-norm on a matrix

$$\|\mathbf{X}(t)\|_2 = \left\| \left[\mathbf{X}(t_1), \mathbf{X}(t_2), \ldots, \mathbf{X}(t_n) \right] \right\|_2. \tag{36}$$

TABLE I
SINGLE-PHASE TRANSFORMER: ERRORS BETWEEN REDUCED AND FULL SOLUTIONS FOR RESISTIVE LOAD SIMULATION.

	$100.\frac{\|i_1^{\text{ref}}-i_1^{\text{mor}}\|_t}{\|i_1^{\text{ref}}\|_t}$	$100.\frac{\|i_2^{\text{ref}}-i_2^{\text{mor}}\|_t}{\|i_2^{\text{ref}}\|_t}$	$100.\frac{\|X^{\text{ref}}-X^{\text{mor}}\|_2}{\|X^{\text{ref}}\|_2}$
Error (%)	1.10	0.42	0.51

TABLE II
SINGLE-PHASE TRANSFORMER: ERRORS BETWEEN REDUCED AND FULL SOLUTIONS FOR RESISTIVE-INDUCTIVE LOAD SIMULATION.

	$100.\frac{\|i_1^{\text{ref}}-i_1^{\text{mor}}\|_t}{\|i_1^{\text{ref}}\|_t}$	$100.\frac{\|i_2^{\text{ref}}-i_2^{\text{mor}}\|_t}{\|i_2^{\text{ref}}\|_t}$	$100.\frac{\|X^{\text{ref}}-X^{\text{mor}}\|_2}{\|X^{\text{ref}}\|_2}$
Error (%)	0.69	0.35	0.39

The errors are compiled in tables I and II: the errors are inferior to 1% on the primary current and even inferior to 0.5% on the secondary current, and less than 1% on the solution vector. The reduced model is able to approximate correctly both global and local values. For that matter the magnetic induction are compared at time $t = 9$ ms corresponding to the maximum nonlinear behaviour onto the current: the fields for full and reduced models along with the difference between the fields are presented figures 6 and 7. Once again we see that the reduced order model is able to simulate the nonlinear behaviour of different load configurations and to be accurate over the local fields.

The magnetic induction B is computed from potential vector A with $B = \nabla \times A$. Vector solution X contains the circulations of A over the edges of the mesh consequently B is obtained on each volume element v by

$$B|_v = \sum_{e \in v} (\nabla \times w_e) X_e, \tag{37}$$

with w_e the edge shape functions associated with the edge e. For the reduced case the formula becomes

$$B|_v \simeq \sum_{e \in v} (\nabla \times w_e) (\mathbf{P}x)_e. \tag{38}$$

To illustrate the contribution of the ROM modes we compute the contribution $B^{(k)}$ of a single vector basis k from $\mathbf{P}$, thus defined

$$B^{(k)}|_v = \sum_{e \in v} (\nabla \times w_e) (\mathbf{P}_{:k})_e, \tag{39}$$

with $\mathbf{P}_{:k}$ the k-th column of $\mathbf{P}$. Figure 8 presents the first four modes of B. The first mode has a physical sense, $B^{(1)}$ gives the main contribution on the magnetic induction. For the next ones, the contribution is local with a maximal magnitude localised in the internal corners where the saturation of the magnetic core is strong.

Table III shows simulation durations which are: 24 minutes, 36 minutes, 63 minutes and 85 minutes for the short-circuit, no-load and loaded full simulations respectively. Regarding the reduced model, less than 13 seconds are needed to read the datas, less than four seconds to compute the basis and the interpolation coefficients and about one minute fifteen seconds to solve the reduced system. Considering only the solving part, the speed-up is between 40 and 60.

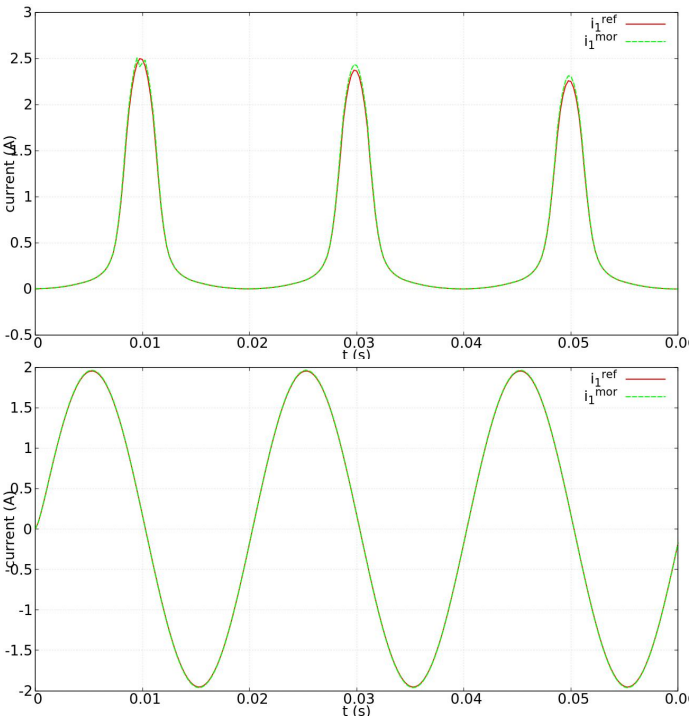

Fig. 4. Single-phase transformer: currents obtained with full and reduced models for no-load and short-circuit cases.

TABLE III
SINGLE-PHASE TRANSFORMER: COMPUTATION DURATIONS FOR THE DIFFERENT SIMULATIONS.

Simulation	Duration
Full model short-circuit	24 min
Full model no-load	36 min
Full model resistive load	63 min
Full model resistive-inductive load	85 min
ROM resistive load	1 min 27 s
ROM model resistive-inductive load	1 min 30 s

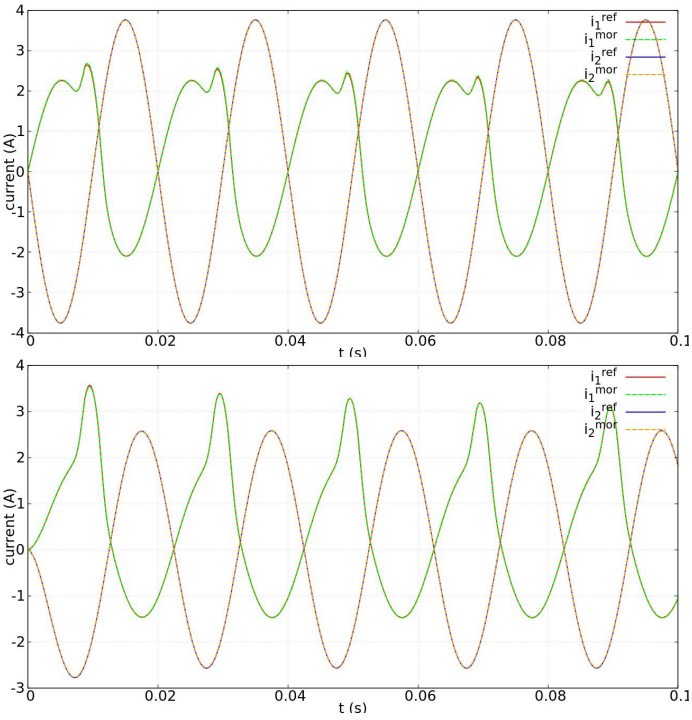

Fig. 5. Single-phase transformer: currents obtained with full and reduced models with resistive load (top) and resistive+inductive load (bottom).

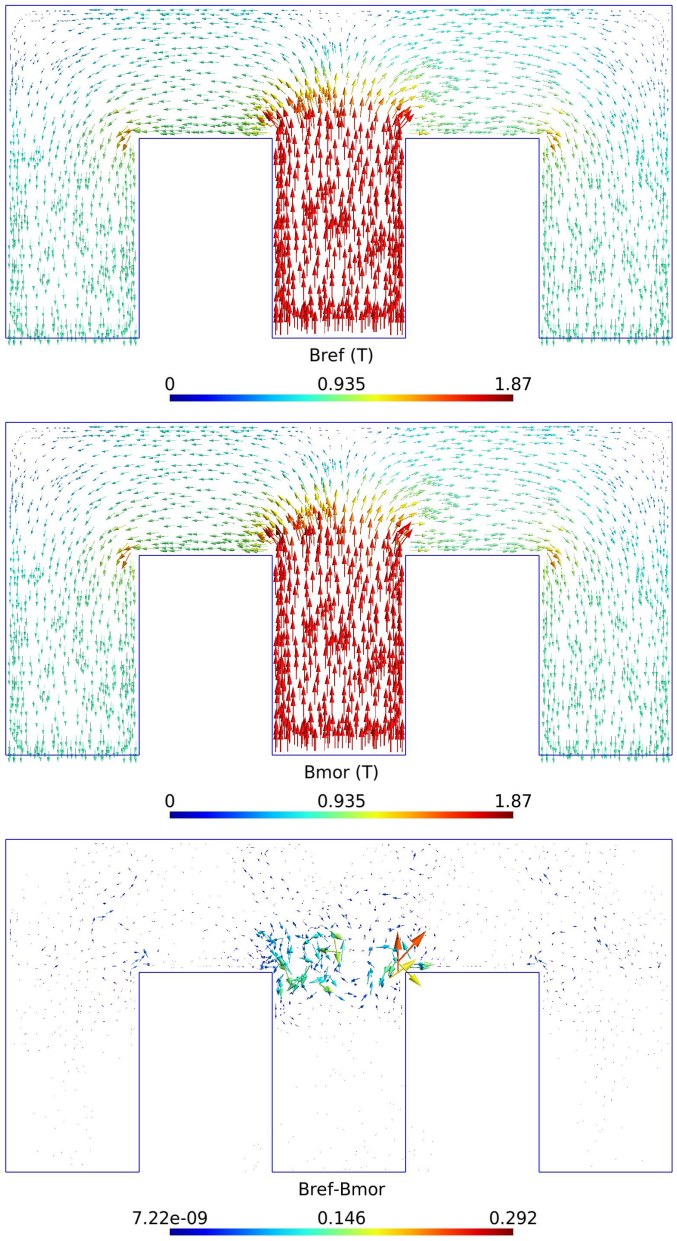

Fig. 6. Single-phase transformer: magnetic induction B (T) obtained with full (Bref) and reduced (Bmor) models with resistive load, and the error between the fields (bottom) at time $t = 9$ ms.

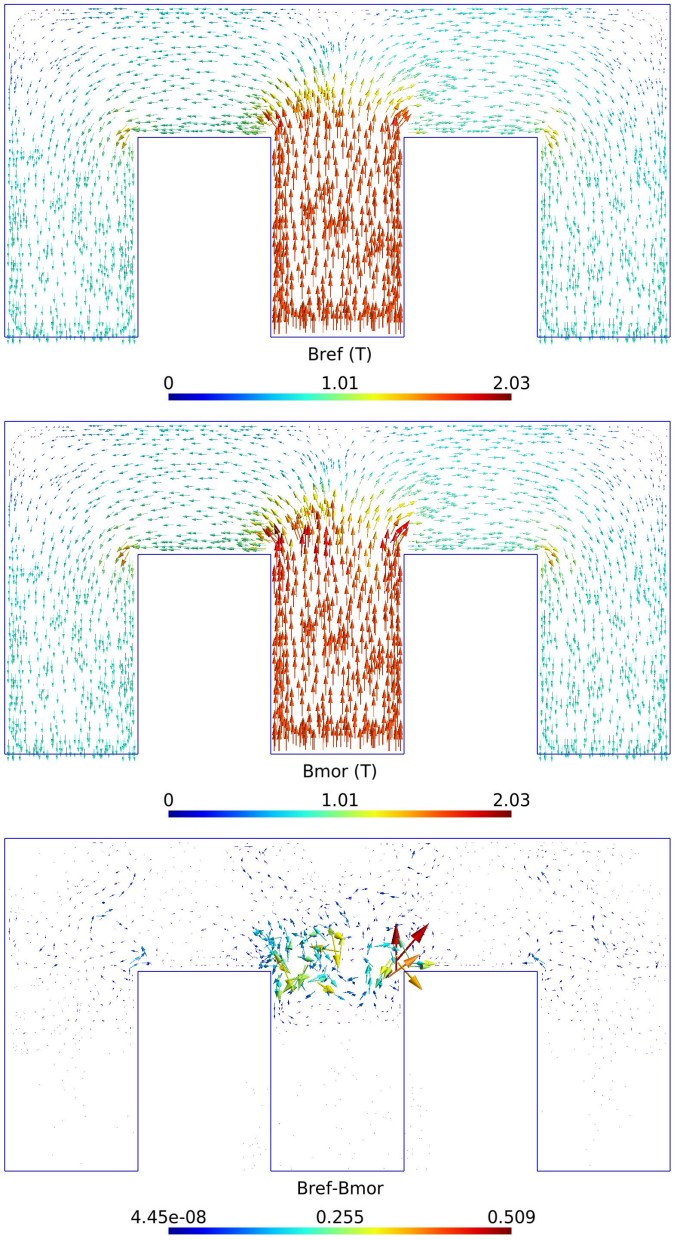

Fig. 7. Single-phase transformer: magnetic induction B (T) obtained with full (Bref) and reduced (Bmor) models with resistive and inductive loads, and the error between the fields (bottom) at time $t = 9$ ms.

B. Three phase transformer

As in previous section the current responses are plotted figure 9 at no-load and in short-circuit. Then the transformer is coupled with balanced resistive loads ($R_c = 30\ \Omega$) on the time window [0,0.12] seconds then with unbalanced resistive loads ($R_c = 30\ \Omega$ but $R_c = 10\ \Omega$ on secondary winding), the currents being available figure 10. The reduced system has 166 unknowns and the RBF interpolation is done with 240 vectors.

The errors are compiled in tables IV and V: the errors are inferior to 10% on the primary current and even inferior to 5% on the secondary current, and less than 2% on the solution vector. The reduced model is able to approximate correctly both global and local values.

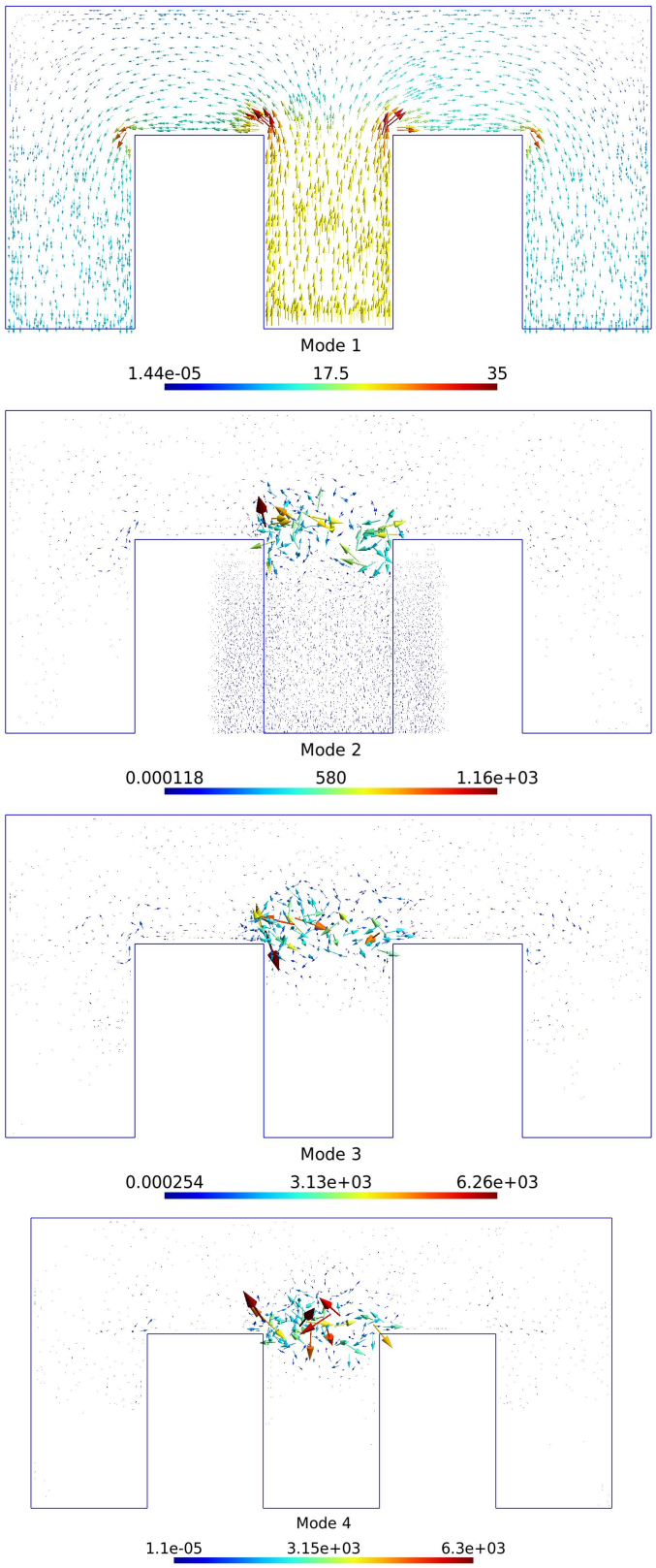

Fig. 8. Single-phase transformer: contribution of the 4 first modes (i.e. the 4 first columns) of the reduced basis P.

TABLE IV
THREE-PHASE TRANSFORMER: ERRORS BETWEEN REDUCED AND FULL SOLUTIONS FOR BALANCED RESISITIVE LOAD SIMULATION.

	Error (%)		Error (%)
$100.\frac{\|i_{11}^{\text{ref}}-i_{11}^{\text{mor}}\|_t}{\|i_{11}^{\text{ref}}\|_t}$	7.94	$100.\frac{\|i_{12}^{\text{ref}}-i_{12}^{\text{mor}}\|_t}{\|i_{12}^{\text{ref}}\|_t}$	0.43
$100.\frac{\|i_{21}^{\text{ref}}-i_{21}^{\text{mor}}\|_t}{\|i_{21}^{\text{ref}}\|_t}$	2.45	$100.\frac{\|i_{22}^{\text{ref}}-i_{22}^{\text{mor}}\|_t}{\|i_{22}^{\text{ref}}\|_t}$	0.21
$100.\frac{\|i_{31}^{\text{ref}}-i_{31}^{\text{mor}}\|_t}{\|i_{31}^{\text{ref}}\|_t}$	2.52	$100.\frac{\|i_{32}^{\text{ref}}-i_{32}^{\text{mor}}\|_t}{\|i_{32}^{\text{ref}}\|_t}$	0.56
$100.\frac{\|X^{\text{ref}}-X^{\text{mor}}\|_2}{\|X^{\text{ref}}\|_2}$	1.53		

TABLE V
THREE-PHASE TRANSFORMER: ERRORS BETWEEN REDUCED AND FULL SOLUTIONS FOR UNBALANCED RESISTIVE LOAD SIMULATION.

	Error (%)		Error (%)
$100.\frac{\|i_{11}^{\text{ref}}-i_{11}^{\text{mor}}\|_t}{\|i_{11}^{\text{ref}}\|_t}$	3.03	$100.\frac{\|i_{12}^{\text{ref}}-i_{12}^{\text{mor}}\|_t}{\|i_{12}^{\text{ref}}\|_t}$	0.35
$100.\frac{\|i_{21}^{\text{ref}}-i_{21}^{\text{mor}}\|_t}{\|i_{21}^{\text{ref}}\|_t}$	2.50	$100.\frac{\|i_{22}^{\text{ref}}-i_{22}^{\text{mor}}\|_t}{\|i_{22}^{\text{ref}}\|_t}$	0.18
$100.\frac{\|i_{31}^{\text{ref}}-i_{31}^{\text{mor}}\|_t}{\|i_{31}^{\text{ref}}\|_t}$	2.02	$100.\frac{\|i_{32}^{\text{ref}}-i_{32}^{\text{mor}}\|_t}{\|i_{32}^{\text{ref}}\|_t}$	0.49
$100.\frac{\|X^{\text{ref}}-X^{\text{mor}}\|_2}{\|X^{\text{ref}}\|_2}$	1.71		

Table VI shows simulation durations which are: 24 minutes, 48 minutes, 86 minutes and 88 minutes for the short-circuit, no-load and loaded full simulations respectively. Regarding the reduced model, less than 13 seconds are needed to read the datas, less than four seconds to compute the basis and the interpolation coefficients and about thirty seconds to solve the reduced system. Considering only the solving part, the speed-up is here between 130 and 180.

TABLE VI
THREE-PHASE TRANSFORMER: COMPUTATION DURATIONS FOR THE DIFFERENT SIMULATIONS.

Simulation	Duration
Full model short-circuit	24 min
Full model no-load	48 min
Full model resistive balanced loads	96 min
Full model resistive unbalanced loads	88 min
ROM resistive balanced loads	44 s
ROM resistive unbalanced loads	32 s

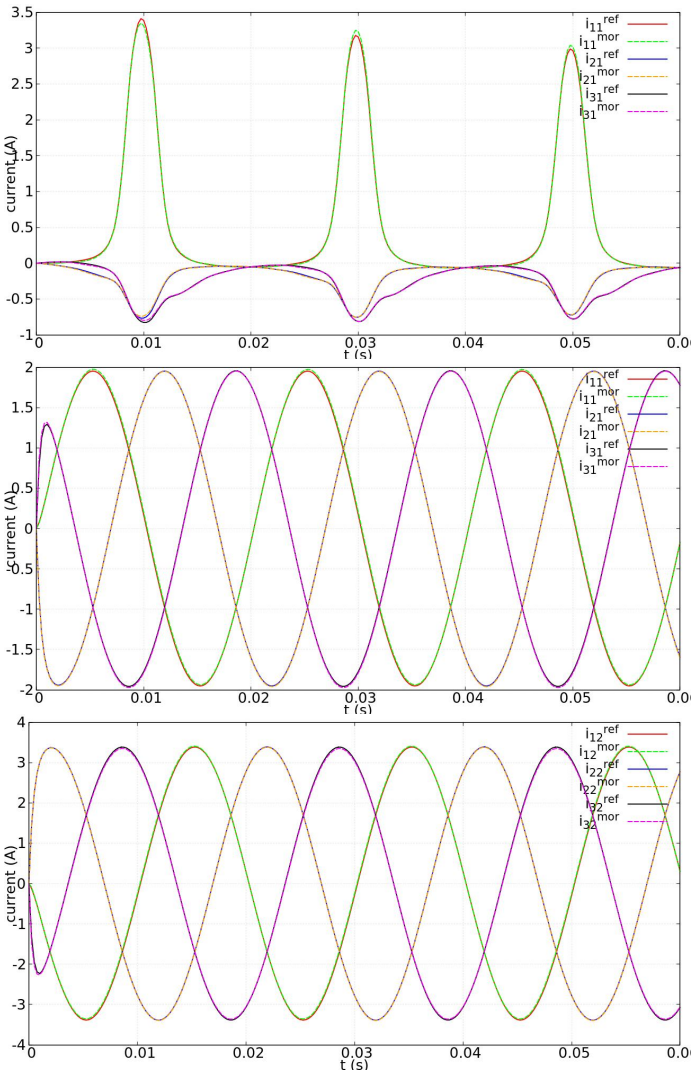

Fig. 9. Three-phase transformer: currents obtained with full and reduced models for no-load and short-circuit cases.

V. CONCLUSION

In order to reduce simulation duration for the modeling of a physical phenomena, two main families of methods exist: model order reduction and metamodel. However most of the reduced order model are intrusives notably in the nonlinear case: on acces to the matrix of the system or to the assembly process is required. To avoid this problem metamodels can be used instead of reduced order model but they are not based on physical formulations so their usage is less adapted in a offline/online strategy or for a multiphysic simulation. On the opposite the data-driven philosophy is to create a reduced model only from the solutions of a problem called snapshots, based on the knowledge of the physical and mathematical formulation. From the solutions a reduced basis is obtained using proper orthogonal decomposition allowing to project the full solutions onto a reduced space. Then through least square problems and radial basis function interpolations a precise and fast reduced order model can be simulated even for a configuration not used for the snapshots. The method is described for magnetostatic problems with a nonlinear

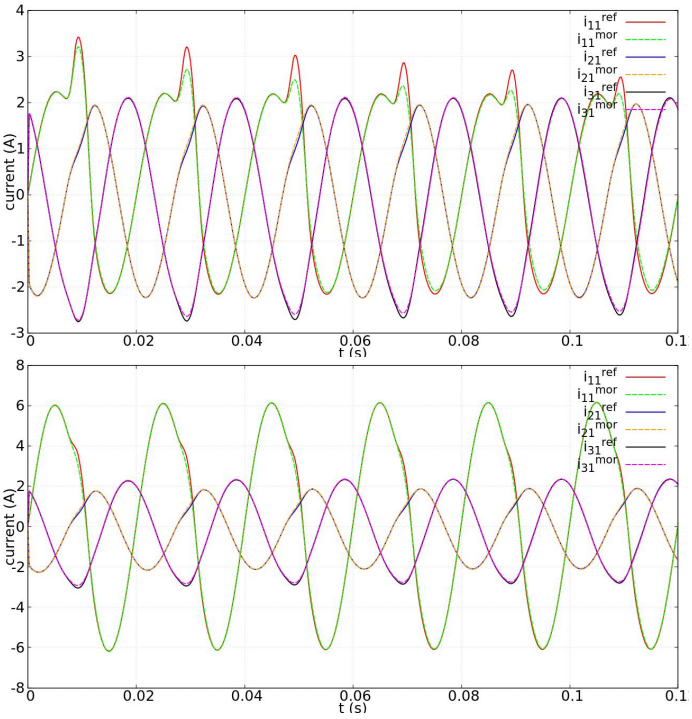

Fig. 10. Three-phase transformer: primary currents obtained with full and reduced models with balanced resistive loads (top) and unbalanced resistive loads (bottom).

magnetic law coupled with time-dependant electric equations. From both application examples, the proposed approach is efficient to simulate fastly a configuration that is not used for the snapshots. In order to improve the solving of the nonlinear reduced order model, the development of an approach allowing to use a Newton method could be considered.

ACKNOWLEDGEMENT

Antoine Pierquin would like to thank the CCIPL (Nantes, France) for providing access to its high-performance computing facilities.

REFERENCES

[1] J.S. Hesthaven, G. Rozza, B. Stamm et al., "Certified Reduced Basis Methods for Parametrized Partial Differential Equations", Springer, 2016.

[2] F. Chinesta, P. Ladevèze, "Separated Representations and PGD-Based Model Reduction. Fundamentals and Applications", CISM International Centre for Mechanical Sciences, Springer, Vienna, 2014.

[3] M. Seoane, P.D. Ledger, A.J. Gil, S. Zlotnik, M. Mallett, "A combined reduced order-full order methodology for the solution of 3D magneto-mechanical problems with application to magnetic resonance imaging scanners", Int J Numer Methods Eng, 121, 3529-3559, 2020.

[4] G. Barroso, M. Seoane, A.J. Gil, P.D. Ledger, M. Mallett, A. Huerta, "A staggered high-dimensional Proper Generalised Decomposition for coupled magneto-mechanical problems with application to MRI scanners", Computer Methods in Applied Mechanics and Engineering, Volume 370, 2020.

[5] G. Barroso, A. J. Gil, P. D. Ledger, M. Mallett, A. Huerta, "A regularised-adaptive Proper Generalised Decomposition implementation for coupled magneto-mechanical problems with application to MRI scanners", Computer Methods in Applied Mechanics and Engineering, Volume 358, 2020.

[6] T. Henneron, S. Clénet, "Application of the Proper Generalized Decomposition to Solve MagnetoElectric Problem", *IEEE Transactions on Magnetics*, Oct. 2017.

[7] Y. Sato, H. Igarashi, "Generation of Equivalent Circuit from Finite-Element Model Using Model Order Reduction", *IEEE Transactions on Magnetics*, 52 (3), no. 1100304, 2016.

[8] Y. Paquay, C. Geuzaine, R. Hasan, R. Sabariego, "Reduced Order Model for Accounting for High Frequency Effects in Power Electronic Components", *IEEE Transactions on Magnetics*, Aug. 2015.

[9] D. Schmidthausler, S. Schops, M. Clemens, "Reduction of linear subdomains for non-linear electro-quasistatic field simulations", *IEEE Transactions on Magnetics*, 49 (5), art. no. 6514566, pp. 1669-1672, 2013

[10] Y. Sato, M. Clemens, H. Igarashi, "Adaptive Subdomain Model Order Reduction With Discrete Empirical Interpolation Method for Nonlinear Magneto-Quasi-Static Problems", *IEEE Transactions on Magnetics*, vol.52, Jan. 2015.

[11] T. Henneron, L. Montier, A. Pierquin, S. Clénet, "Comparison of DEIM and BPIM to Speed up a POD-based Nonlinear Magnetostatic Model", *IEEE Transactions on Magnetics*, Vol. 53, N. 6, june 2017.

[12] B. Peherstorfer, K. Willcox, "Data-driven operator inference for non-intrusive projection-based model reduction", *Computer Methods in Applied Mechanics and Engineering*, 306, pp. 196-215, 2016.

[13] B. Peherstorfer, K. Willcox, "Dynamic data-driven model reduction: adapting reduced models from incomplete data", *Advanced Modeling and Simulation in Engineering Sciences*, 3 (1), no. 11, 2016.

[14] V. Singh, K. Willcox, "Methodology for path planning with dynamic data-driven flight capability estimation", *AIAA Journal*, 55 (8), pp. 2727-2738, 2017

[15] A. Pierquin, T. Henneron, S. Clénet, "Data-Driven Model Order Reduction for Magnetostatic Problem Coupled with Circuit Equations", *IEEE Transactions on Magnetics*, March 2018.

[16] S. Jakobsson, B. Andersson, F. Edelvik, "Rational radial basis function interpolation with applications to antenna design", *Journal of Computational and Applied Mathematics*, vol. 233, issue 4, pp. 889-904, 2009.

[17] M. Urquhart , E. Ljungskog, S. Sebben, "Surrogate-based optimisation using adaptively scaled radial basis functions", Applied Soft Computing Journal, 2020.

[18] T. Henneron, A. Pierquin, S. Clénet, "Surrogate Model Based on the POD Combined With the RBF Interpolation of Nonlinear Magnetostatic FE Model", *IEEE Transactions on Magnetics*, vol. 56, no. 1, pp. 1-4, Jan. 2020.

[19] T. Henneron, S. Clénet, "Model-Order Reduction of Multiple-Input Non-Linear Systems Based on POD and DEI Methods", *IEEE Transactions on Magnetics* vol. 51, no. 3, april 2015.

[20] L. Montier, T. Henneron, S. Clénet, B. Goursaud, "Transient simulation of an electrical rotating machine achieved through model order reduction", *Advanced Modeling and Simulation in Engineering Sciences*, vol. 3, no. 10, march 2016.

[21] F. Piriou, A. Razek, "A non-linear coupled 3D model for magnetic field and electric circuit equations", *IEEE Transactions on Magnetics* vol. 28, no. 2, pp. 1295-1298, March 1992.

[22] F. Piriou, A. Razek, "Finite element analysis in electromagnetic systems-accounting for electric circuits", *IEEE Transactions on Magnetics*, vol. 29, no. 2, pp. 1669-1675, March 1993.

[23] J. Gyselinck, P. Dular, N. Sadowski, J. Leite and J.P.A Bastos, "Incorporation of a Jiles-Atherton vector hysteresis model in 2D FE magnetic field computations: Application of the Newton-Raphson method", COMPEL - The international journal for computation and mathematics in electrical and electronic engineering, Vol. 23 No. 3, pp. 685-693, 2004.

[24] C. Geuzaine and J.-F. Remacle, "Gmsh: a three-dimensional finite element mesh generator with built-in pre- and post-processing facilities", *International Journal for Numerical Methods in Engineering*, 79(11), pp. 1309-1331, 2009.

[25] C. Geuzaine, "GetDP: a general finite-element solver for the de Rham complex", PAMM Volume 7 Issue 1. Special Issue: Sixth International Congress on Industrial Applied Mathematics (ICIAM07) and GAMM Annual Meeting,Zürich 2007.

[26] M. Frăţilă, "Contribution à la prise en compte des pertes fer dans la modlisation des machines électriques par éléments finis", PhD thesis (in french), pp. 85, univ. Lille, 2012.